

Monitoring of Tissue Perfusion and Cellular Function

M. Kessler, M.D., J. Höper, M.D., B. A. Krumme, M.D.

RECENT ADVANCES in the development of electrodes have opened a new field for investigation of physiologic processes by direct monitoring of specific signals obtained from the tissues. The details are described in several recent monographs.^{1,2,4,6,11,23,26} These new "tools" will allow recording of pathophysiologic alterations in the patient, while the "new cuvettes" used in the diagnosis are the capillaries, the extracellular space, and the individual cells.

Methodology

ELECTRODES FOR MEASUREMENT OF TISSUE P_{O_2} AND P_{H_2}

These electrodes are used for the measurement of oxygenation (P_{O_2}) and blood flow (P_{H_2} washin and washout) in various tissues. The determinations can be made with either surface or needle-type electrodes.

Multiwire surface electrodes of the Clark type,² developed in our laboratory,¹⁸⁻²⁰ have proved of value in basic research and in clinical practice for monitoring local oxygen supplies and blood flows in the microcirculations of various tissues and organs (fig. 1). Data have been collected from the kidneys^{46,49} of patients at operation.

Micro-needle polarographic electrodes for P_{O_2} and P_{H_2} measurements^{4,7,9,29,50,56} have achieved great importance as tools for basic research. Compared with Clark-type electrodes, which are protected by inert membranes, the function of micro-tip electrodes can be disturbed more easily by the presence of different ions, protein concentration, and electrical noise. Furthermore, they must be

handled with extreme care to prevent breakage of the thin tips, and their application in clinical medicine is still very limited.

Features of the multiwire surface electrode ("Dortmund-type") developed in our laboratory are as follows:

- 1) Oxygen or hydrogen tension can be monitored continuously and simultaneously at eight to 16 different points within tissues.

- 2) Weight of the electrode is such that it can be supported by the tissue without the risk of ischemia due to excessive pressure on the capillaries being monitored.

- 3) The electrode can be adapted with a flange and secured to the tissue by means of wet cellophane or a piece of wet felt (see fig. 1).

- 4) Signals from the electrode are transmitted via thin, flexible Teflon-insulated wires. This enables us to obtain precise recordings of the local oxygen or hydrogen tensions despite motion of the functioning organ.

Measurement of Oxygen Tension

At a polarization voltage of -700 mV, the single platinum wire (diameter: $15\text{ }\mu\text{m}$) of the electrode, registers a reduction current of 1 to 2×10^{-9} amps/100 mm Hg. The calibration curve is linear. Drift of the signal is approximately 5 per cent per hour. The radius of the hemispheric surface area of the different platinum wires is $20-25\text{ }\mu\text{m}$ when a membrane $25\text{ }\mu\text{m}$ thick is used. Under these conditions, convection sensitivity is 3 to 4 per cent and the 95 per cent response time is 3 to 4 seconds.

Measurement of Hydrogen Tension

For the recording of hydrogen tension (P_{H_2}), the platinum wires must be palladized.^{31,39} Voltage used for the polarographic oxidation of hydrogen lies within a range of $0-100$ mV. A hydrogen tension (P_{H_2}) of 100 mm Hg generates a current of 1 to 2×10^{-9} amps. Drift of the electrode is approximately 5 per cent per hour.

Received from the Max-Planck-Institut für Systemphysiologie, Dortmund, GFR. Supported by a grant of the Ministerium für Wissenschaft und Forschung des Landes Nordrhein-Westfalen.

Address reprint requests to Dr. Kessler: Max-Planck-Institut für Systemphysiologie, 46 Dortmund, Rheinlanddamm 201, Federal Republic of Germany.

Recording Instrumentation

A multichannel polarization voltage and a multichannel amplifier unit are used in combination with an automatic data logger consisting of a scanner, an AD-converter, an electronic clock, a serializer, and a magnetic tape (MIT-P₀₂-system) (Mess-Instrumente-Technik, Friedenspromenade 40, 8000 München, GFR). P₀₂ and P_{H2} signals are recorded on a multichannel recorder. The tape-recorded digital data are evaluated by a computer, which corrects for drift of the electrodes, and plots the histograms as well as the resulting P₀₂ and P_{H2} curves. If on-line computer facilities are available, direct evaluation of the digitalized data is possible.

ELECTRODES FOR MEASUREMENT OF TISSUE POTASSIUM, SODIUM, CALCIUM, AND PROTON ACTIVITY

Measurement of Ionic Activity

Ion-selective electrodes have been developed for measurement of tissue pK, pNa, pCa, and pH.^{15,26-29} Sodium- and calcium-selective electrodes have become available as a result of the pioneering work by Simon and colleagues^{1,2,20,26} from the Laboratory of Organic Chemistry at the Federal Institute of Technology in Zürich, who were able to synthesize new ligands with high selectivity for sodium and calcium ions.^{1,2,20} Incorporation of these new lipophilic ligands and valinomycin into polyvinylchloride (PVC)¹² has resulted in membranes with high selectivity for sodium, potassium, and calcium. Single and multiple solid-state surface electrodes for tissue measurements have been constructed.^{15,26,28} Measurements obtained from the surfaces of brain, liver, kidney, and skeletal muscle have indicated that they monitor the extracellular cation activities of different tissues with great accuracy. The principle of construction for a typical liquid membrane surface electrode is shown in figure 2. A silver wire is glued into a small PVC cylinder, and the silver tip is coated with a ligand-impregnated PVC membrane. Treatment of the silver surface with tetraphenylborate and addition of tetraphenylborate to the membrane phase²³ result in a very stable, solid electrode. Drift is approximately 0.1

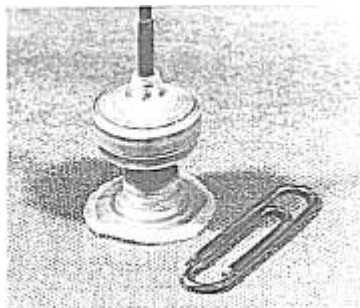


FIG. 1. Multichannel surface electrode for measurement of P₀₂ or P_{H2} in tissue.

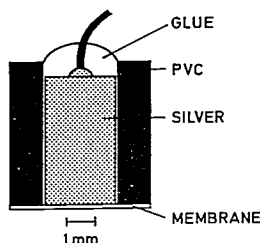


FIG. 2. Diagram of ion-selective electrode (solid-state) for measurements of K⁺, Na⁺, and Ca⁺⁺ on the surfaces of tissues.

mV/hour. For a given set of experimental conditions, 90 per cent of the final signal amplitude is attained within 5 to 10 seconds. Silver chloride is used as a reference electrode. Absolute potential of this measuring circuit amounts to about 50 mV in 100 mM solutions. Slopes of the K⁺ and Na⁺ electrodes lie within the range of 54–58 mV/logarithmic activity unit and that for the Ca⁺⁺ electrode, within 24–26 mV/logarithmic activity unit. The selectivity data have been reported recently.²⁰ For pH measurements we use pH-sensitive glass membranes or needles.^{27,29}

Recording Instrumentation

Measurement of the electromotive forces (EMF) generated by different ion activities at and within the ion-specific membranes of the

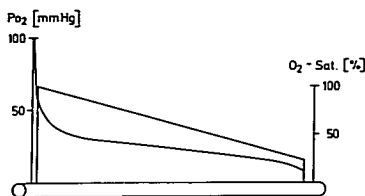


FIG. 3. Slope of P_{O_2} (measured values) and oxygen saturation along the sinusoid of rat liver. Arterialized end at left, venous at right.

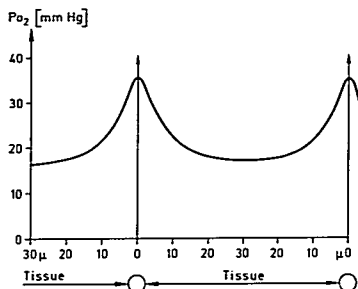


FIG. 4. Calculated field of oxygen tension between two brain capillaries. The latter are shown as two open circles below the X-axis. (See also Thews.²³)

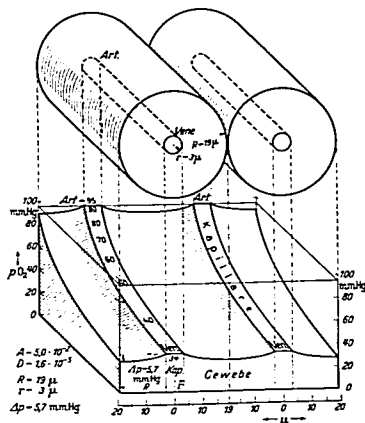
electrodes is obtained with a multichannel amplifier system and a differential input, originally developed in our laboratories. The input impedance of the ion-specific electrode channel is $>10^{13} \Omega$, and the ionic activities can be recorded simultaneously as pNa , pCa , pK , and pH values and as mM or mEq values. Patterns of ionic activity are registered on a multichannel recorder. Digital evaluation of the data is possible with equipment similar to that described for the P_{O_2} and P_{H_2} electrodes.

Experimental Considerations

TISSUE PERFUSION AND OXYGEN SUPPLY

Krogh first published his ingenious concept of the three-dimensional distribution of oxygen tension in tissue in 1919.²⁴ Based on his

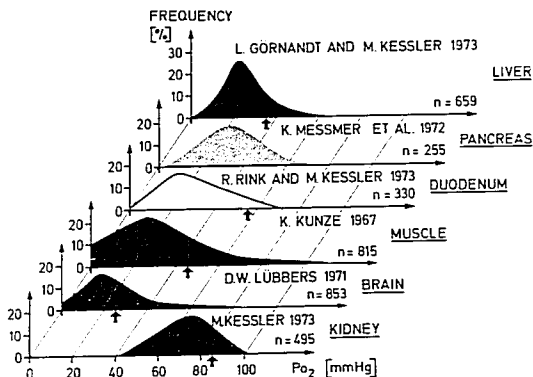
experimental data and a theoretical model that consisted of a system of parallel capillaries and their surrounding cells, he developed a system to deal with gas-exchange problems when oxygenation (P_{O_2}) and blood flow were altered. It became known, subsequently, as the "Krogh cylinder." Experimental evidence to support the model as an appropriate first approximation of the physiologic situation has become available only in the past 15 years. Figure 3, based on these data,¹⁰ shows the mean decrease of P_{O_2} along liver sinusoids as O_2 is taken up by liver cells. The decrease in P_{O_2} , the result of diffusion from hemoglobin in the erythrocytes to the mitochondria in the surrounding cells, is non-linear, whereas the decrease in oxygen saturation along the capillary is linear. The P_{O_2} profile between adjacent brain capillaries as induced by diffusion of oxygen is also non-linear (fig. 4). Although the practical aspects of this problem are of utmost importance, our understanding must still rely heavily on the theoretical model, since data on intercapillary P_{O_2} gradients are not available. When the two gradients along and be-



Opitz und Schneider 1950

FIG. 5. Three-dimensional distribution of O_2 within two parallel Krogh cylinders. (Reproduced with permission from Opitz and Schneider.¹⁴)

FIG. 6. Frequency distribution of oxygen tensions in different organs. Data obtained from different authors as shown.



tween capillaries are used to construct a three-dimensional Krogh model,¹⁴ it becomes evident that a spatial and therefore inhomogeneous tissue distribution of P_{O_2} must exist (see fig. 5). The results of experiments performed to study tissue oxygen supplies in different organs are shown in figure 6. P_{O_2} frequency distribution curves, or so-called P_{O_2} histograms, were obtained for different organs following several hundred tissue P_{O_2} measurements.

Inspection of figure 6 indicates the following points not predicted by the Krogh model:

- 1) The lowest P_{O_2} values are below those found in the so-called lethal corner¹¹ located between two capillaries at the venous end of the Krogh cylinders.

- 2) Maxima of the P_{O_2} histograms are fairly low, or in a range of 15 to 30 mm Hg. An exception is the outer cortex of the kidney, an organ with a high functional blood flow.

- 3) The venous blood P_{O_2} is not indicative of the low tissue P_{O_2} values and lies above the maxima found in the P_{O_2} histograms.

- 4) Despite great variability in capillary architectures, magnitudes of blood flow, and O_2 uptakes, P_{O_2} histograms recorded from different organs reveal a surprising monotonic similarity.

Homogeneity of the P_{O_2} histograms demonstrates that under physiologic conditions, organ oxygen supply is controlled precisely by a

very efficient system. Data identifying these controls are needed. Since the critical mitochondrial P_{O_2} appears to be below 0.1 mm Hg²¹ and since tissue P_{O_2} approaches this value, we must also conclude that O_2 utilization is subject to very efficient optimization. In fact, a contradiction is apparent between the optimized utilization of oxygen in the tissues and the recorded higher venous blood P_{O_2} values. The latter imply that from a practical standpoint, cardiac output normally exceeds the effective requirement for oxygenated blood by an estimated 50 per cent of total flow, and suggest that maintenance of a high venous blood P_{O_2} is part of an important regulatory system for the intact organism.

REDISTRIBUTION OF MICROCIRCULATION

Experiments performed by Kessler *et al.*²¹ have indicated that an important aspect of tissue regulation to protect against hypoxemia may reside in the ability for redistribution of blood flow within the microcirculation. According to Suwa and Takahashi,²⁴ tissue capillaries are inhomogeneous in length, a pattern that appears to result in an inhomogeneous distribution of capillary blood flow. An example of length frequency distribution in rat liver sinusoids is shown in figure 7. We have also included calculations of micro-flow (expressed in per cent of control) for dif-

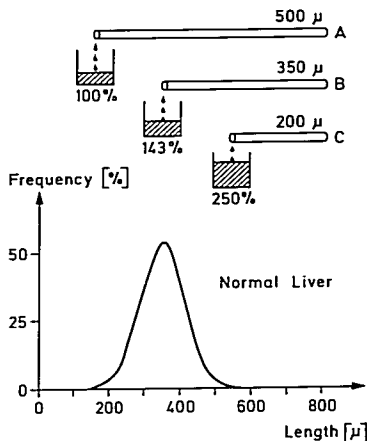


FIG. 7. Length frequency distribution curve for liver sinusoids as described by Suwa and Takahashi.²³ Upper portion of the figure indicates the magnitude of calculated flow (in per cent) as the capillary lengths are reduced from 500 to 200 μ m.

ferent capillary lengths according to the Hagen-Poiseuille relationship.

Krumme *et al.*^{24,25} have estimated liver microflow in anesthetized rats by measurement of H_2 -washout following saturation with an inspired gas mixture of 20 per cent O_2 , 5 per cent H_2 , and 75 per cent N_2 . The measurements obtained with H_2 -sensitive multiwire electrodes are summarized in figure 8. The data, which indicate a pattern of inhomogeneous microflow, are compared in the upper part of the figure with our calculations, again assumed on the basis of low, intermediate and high values for microflow present in sinusoids of different lengths. Comparison of the theoretical data from figure 7 with those of figure 7 reveals a remarkable similarity. This is particularly surprising in view of the fact that capillary diameter, an important determinant of flow, was not taken into account because exact measurements were not possible *in vivo*.

Inhomogeneity of capillary length and blood flow distribution within the microcirculation has been shown to result in a high mixed

venous blood P_{O_2} .²⁴ This finding raises the possibility that the venous blood " O_2 reserve" can be utilized for redistribution of flow in the microcirculation whenever O_2 requirements are increased. Measurements performed with P_{O_2} and P_{H_2} electrodes have demonstrated that such redistribution can indeed be induced by several stimuli, including arterial hypoxemia and drugs, and that this mechanism can, within limits, prevent the consequences of tissue oxygen lack. For example, Krumme *et al.*^{24,25} have evaluated changes in the rat liver *in situ* during arterial hypoxemia with and without the addition of a potent vasoconstrictor such as norepinephrine. Changes in the sinusoid blood flow were evaluated in three regions characterized as having "high," "normal," and "low" blood flows (fig. 9). A reduction in the inspired O_2 concentration reduced blood flow by 21.2 per cent in the "high"-flow and only 7.2 per cent in the "low"-flow sinusoids. In contrast, addition of norepinephrine (fig. 10) increased flow in the "low"-flow region by 21.6 per cent, and decreased it in the "high"-flow region by 20.7 per cent. These data suggest that measurements of global blood flow are in no way indicative of the distribution of blood within an organ, and point to the need for more specific monitoring within organs of both flow distribution and metabolic activity.

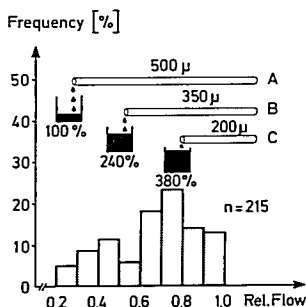


FIG. 8. Frequency distribution curve of microflow rates for rat liver *in situ*. On the upper part flow was calculated for three lengths of capillaries on the assumption that a 500- μ m length was representative for a flow of 100 per cent.

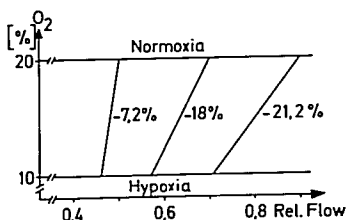


FIG. 9. The effect of hypoxemia on blood flow produced by lowering the inspired O_2 concentration from 20 to 10 per cent was evaluated in the sinusoids of the rat liver by the technique of hydrogen clearance. The analysis was made for three regions, indicated from left to right by the three vertical or slanted lines. Low flow at left and high flow at right. A reduction in the inspired O_2 concentration reduced blood flow in the "low-flow" region by 7.2 per cent and that in the "high-flow" region by 21.2 per cent.

INSUFFICIENCY OF TISSUE PERFUSION AND/OR OXYGEN SUPPLY

When a compensatory factor such as an increase of organ blood flow, a redistribution of flow at the microcirculation level, or a decrease in oxygen uptake¹⁸ does not suffice to secure local oxygen demand, several pathologic situations may develop. We can characterize them as follows (see fig. 11): 1) Normal-flow (100 per cent) anoxia (A) at end-capillaries caused by arterial hypoxemia; 2) High-flow (200 per cent) anoxia (B) at end-capillaries due to a decrease in O_2 capacity

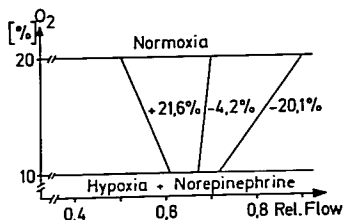


FIG. 10. The effect of hypoxemia plus administration of norepinephrine on blood flow when inspired O_2 decreased from 20 to 10 per cent. Measurements were made in the sinusoids of the rat liver. Symbols are the same as in figure 9. In contrast to hypoxemia alone, addition of norepinephrine increased blood flow in the "low-flow" region by 21.6 per cent.

secondary to anemia or extreme hemodilution^{31,32}; 3) Low-flow (70 per cent) anoxia (C) at end-capillaries due to vasoconstriction, decrease in cardiac output, or rheologic disturbance; 4) No-flow (0) anoxia (D) at end-capillaries due to cessation of blood flow secondary to embolization, edema, etc. Clinically inadequate oxygenation is often the result of a combined effect.

DISTURBANCES OF TISSUE PERFUSION AND OF LOCAL OXYGEN SUPPLY SECONDARY TO HEMORRHAGE

Measurements made during hemorrhage have shown that local skeletal muscle oxygen supply is disturbed at an early stage following

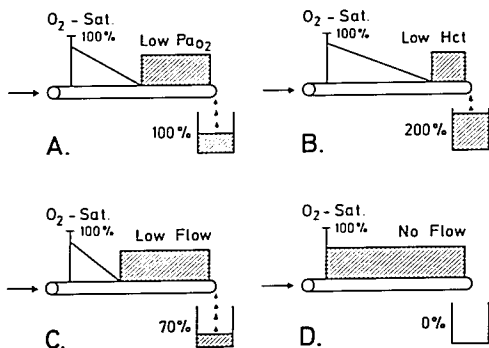


FIG. 11. Types of tissue anoxia. Cross-hatched area indicates segment of capillary subjected to a critically low P_{aO_2} .

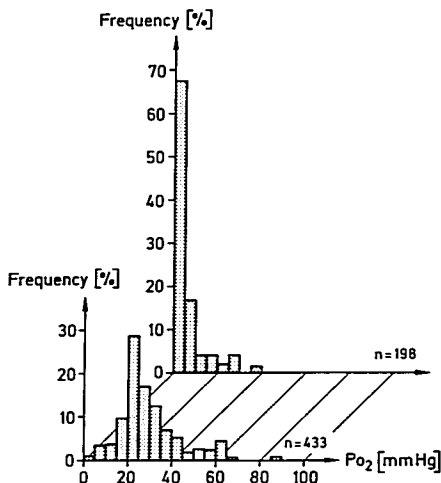
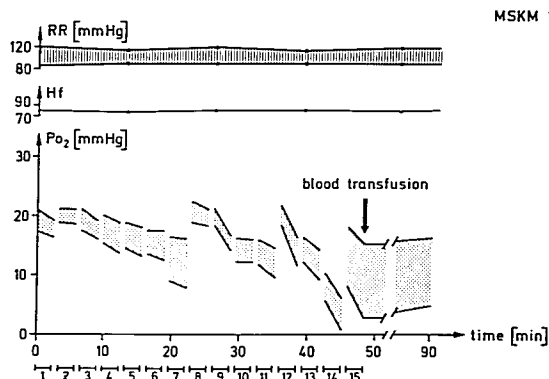


FIG. 12. P_{O_2} histograms in dog skeletal muscle before (lower) and during (upper) hemorrhagic shock. (Reproduced with permission from Sinagowitz *et al.*⁵¹)

hemorrhage when blood gases, arterial blood pressure, and central venous pressure are still within the normal range.^{21,46,51} Comparison of tissue P_{O_2} measurements with other direct methods, such as photometric techniques and hydrogen clearance, has shown that estimation of the P_{O_2} histogram is still the most accurate method for analysis of the microcir-

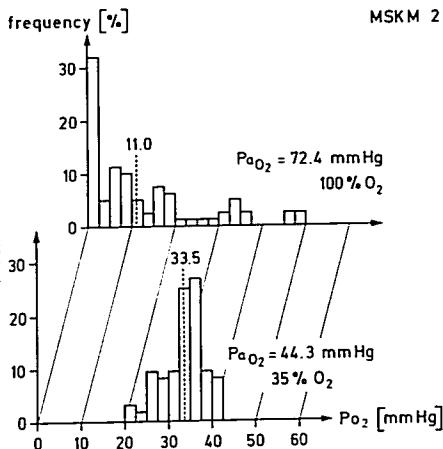
culation. Although the P_{O_2} histogram does not allow conclusions based on absolute numbers, it does tell us whether the microcirculation is disturbed or not. A "physiologic" histogram implies that the demands placed upon the microcirculation compared with oxygen demands of the tissues have not been excessive. When the microcirculation is disturbed, the



MSKM 1

FIG. 13. Oxygen tensions measured in skeletal muscle of a patient during gastrointestinal bleeding and concomitant blood transfusion. Upper and lower limits of P_{O_2} readings from a multiwire electrode are shown. Arterial blood pressure (RR) and heart rate (HF) are shown in the upper portion of the graph. (Reproduced with permission from Schönleben *et al.*⁴⁶)

FIG. 14. P_{O_2} histograms of skeletal muscle in a patient during mechanical ventilation with 100 per cent O_2 and with 35 per cent O_2 . Mean muscle P_{O_2} increased from 11 mm Hg during ventilation with 100 per cent O_2 to 44.3 mm Hg during ventilation with 35 per cent O_2 , probably due to redistribution of flow in the microcirculation.



histogram assumes an irregular shape, with several peaks and shifts to low mean P_{O_2} values. A typical example of a disturbance induced by hemorrhage in the dog is shown in figure 12.^{51,52} The distribution curve has shifted to the left. However, even under these conditions, the data reveal that portions of the tissues may still be normally supplied with oxygen. Figure 13 shows values obtained in skeletal muscle of a patient treated in the intensive care unit following partial pancreatectomy.⁴⁶ The local P_{O_2} measurements were made with a multiwire electrode placed at several positions (each recording consisted of eight readings); the figure indicates the highest and the lowest P_{O_2} values for each set of readings. The gradual decrease in muscle P_{O_2} was partially reversed by blood transfusion, but muscle P_{O_2} remained below normal (see figure 12 for frequency distribution) until, at 90 minutes, the patient had a substantial hematemeses due to a stress ulcer. In retrospect, the tissue P_{O_2} readings were indicative of a compromised circulation despite apparently adequate vital signs and what was thought to be appropriate blood-volume replacement. As shown recently,¹⁷ an increase in intraluminal pressure of the ileum also can cause severe disturbances of local tissue oxygen supply.

DISTURBANCES OF TISSUE PERFUSION INDUCED BY HYPEROXIA IN INSPIRED AIR

An excessively high oxygen concentration in the inspired air can cause marked changes

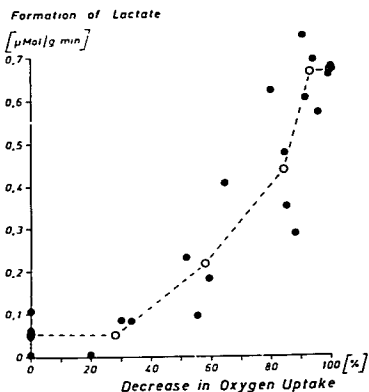


FIG. 15. Relationship between the decrease in oxygen uptake and lactate formation in the perfused rat liver. A substantial increase in lactate appears when O_2 uptake has decreased by 50 per cent.

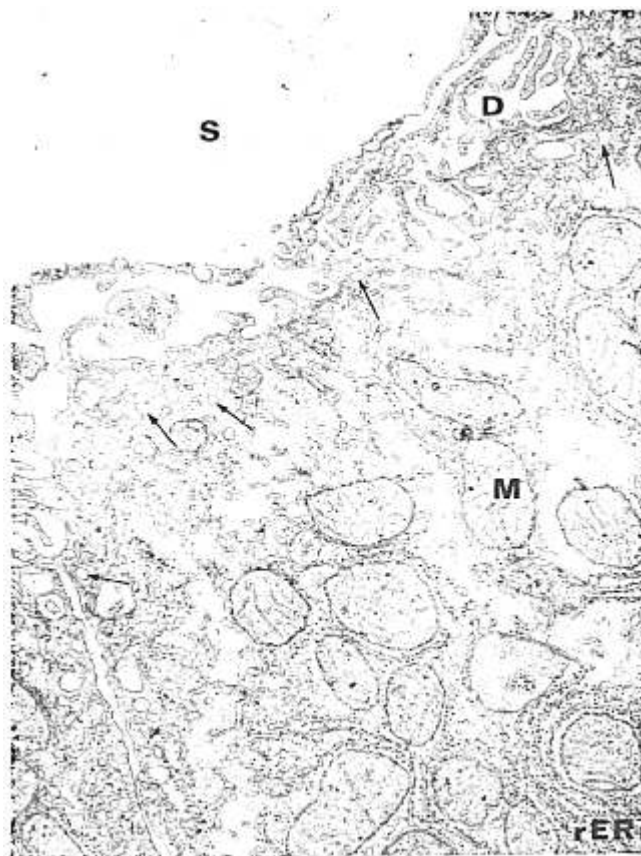


FIG. 16. Section of rat liver after anoxia for an hour (perfusion fixation: 0.2M glutaraldehyde + 0.2M sucrose in 0.1M cacodylate buffer, pH, 7.4 and 580 mOsm for 10 min). Small vacuoles (arrows) are seen in the cytoplasm, especially near the space of Disse (D). There are slight, localized swellings in the cristae of the mitochondria. S = sinusoid. Magnification, 30,000 \times .

in the microcirculation. This was seen during skeletal muscle monitoring with multiwire P_{O_2} electrodes in critically ill patients* (fig. 14).

* Observations in patients treated in the intensive care unit were made in collaboration with Dr. Schönleben and Prof. Bünte from the Department of Surgery of the University of Münster.

The findings of these studies can be summarized as follows:

- 1) The threshold for a change in tissue P_{O_2} lies within a narrow range between high and low inspired O_2 concentrations. For example, an inspired O_2 concentration of 30 per cent may be optimal, while values below 21 per

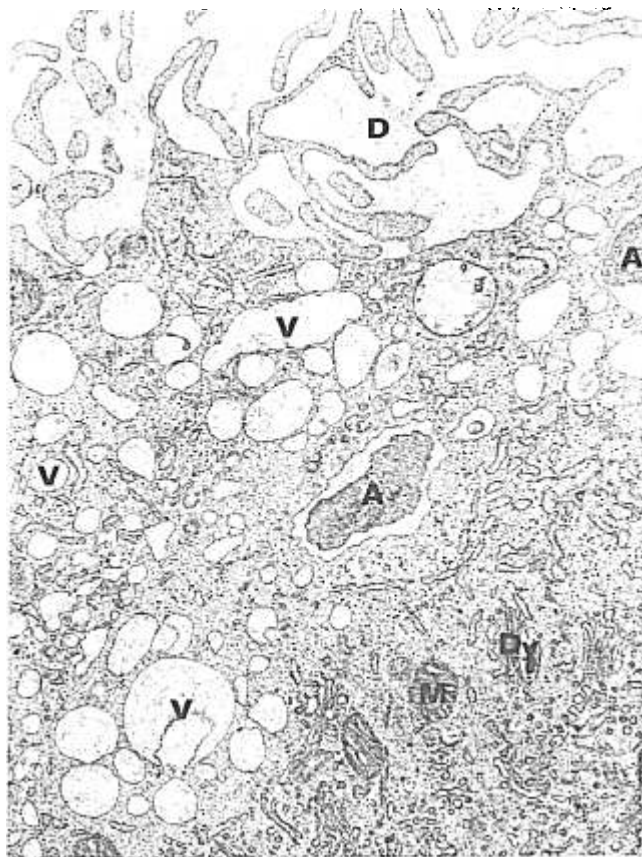


FIG. 17. View of rat liver obtained after 10 minutes of ischemia (*i.e.*, no-flow anoxia). Many large vacuoles (V) are present in the cytoplasm of hepatocytes close to the spaces of Dissé (D). The latter are distinctly enlarged. The number of autolysosomes (A) is increased, while the distosomes (Dy) of the Golgi apparatus appear shortened and show partial enlargement. The intercrystal spaces of the mitochondria are somewhat distended. Magnification, 30,000 \times .

cent and above 40 per cent may result in marked alterations of the local oxygen supply. Similar results have been recorded in the beating rat heart.^{3,13} The effect is probably mediated via changes in intercapillary dis-

tance secondary to the effect of O₂ on sphincters that control blood flow.

2) Adequacy of tissue oxygenation cannot be predicted solely from measurement of arterial blood P_{O₂} since "normal" values

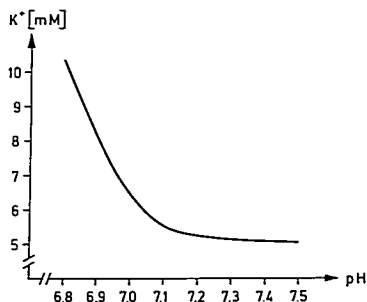


FIG. 18. Correlation between extracellular pH and potassium efflux during no-flow anoxia.

may be associated with an inadequate tissue supply.

OXYGEN LACK AND ANAEROBIC GLYCOLYSIS

Whenever compensating mechanisms do not provide the tissues with sufficient oxygen, anaerobic glycolysis develops.⁴⁷ In studies performed in the isolated, perfused organ (*i.e.*, rat liver), reduction in O_2 supply resulted in prompt decreases in O_2 uptake and respiratory enzyme activity. Most important from the usual monitoring point of view, lactate formation increased slowly at first (fig. 15), while the lactate/pyruvate ratio increased only when O_2 uptake had decreased by 60 to 70 per cent.^{16,22,27,28}

ULTRASTRUCTURAL ALTERATIONS DURING NORMAL-FLOW AND NO-FLOW ANOXIA

In agreement with observations made in the isolated, perfused rat liver during normal-flow anoxia, ultrastructural analyses reveal no severe damage.²⁹ After one hour of normal-flow anoxia (*i.e.*, blood flow with a very low P_{O_2}), small vacuoles are found in the cytoplasm of the hepatocytes. Slight local edema can be observed within the intracisternal spaces of the mitochondria (see fig. 16).

After no-flow anoxia for 10 minutes initiated by cessation of perfusion, drastic alterations can be demonstrated by electron microscopy (fig. 17).

In summary, normal-flow anoxia for an hour

causes only slight morphologic alterations, whereas no-flow anoxia (ischemia) for 10 minutes results in pronounced cellular damage.

IONIC DISTURBANCES DURING NORMAL-FLOW AND NO-FLOW ANOXIA

During normal-flow anoxia, extracellular hydrogen (protons), sodium, potassium, and calcium ionic activities were measured with ion-selective surface and needle electrodes. The two types of electrodes delivered comparable results. Alterations of ionic activity during normal-flow anoxia (pK , pNa , pCa) were negligible both in tissue (liver) and in the perfusate.³² Immediately after cessation of perfusion, extracellular pH decreased, and 10 minutes after the onset of no-flow anoxia, intracellular pH was reduced to 6.5. When the extracellular pH fell below 7.1, potassium efflux became very prominent (fig. 18). The pattern of sodium and potassium exchange induced by no-flow anoxia is shown in figure 19.

Experiments performed during no-flow anoxia at different levels of extracellular calcium activities have shown a significant correlation between ischemic potassium efflux and extracellular calcium activity (fig 20).¹⁴

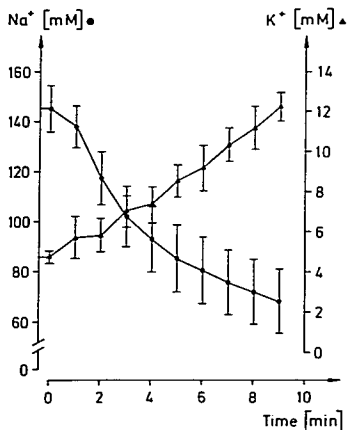


FIG. 19. Extracellular sodium and potassium activities on the surface of perfused liver after the beginning of no-flow anoxia.

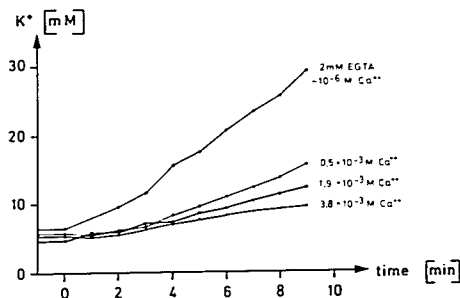


FIG. 20. Potassium efflux of perfused liver during no-flow anoxia as a function of extracellular calcium activity.

Also, during no-flow anoxia, extracellular calcium activity, as monitored with the calcium electrode, increases initially and finally decreases. This may represent the point when calcium ions penetrate the cellular membrane to act as "killer ions" and induce cellular necrosis. Similar, although not identical, disturbances have been observed in other organs, such as the kidney and skeletal muscle. In the kidney, 10 minutes after the onset of ischemia, an increase in extracellular potassium activity to 32.7 mM and a decrease in sodium activity to 89.7 mM can be detected with ion-selective electrodes, while calcium activity increases only from 1.7 to 2.2 mM. In skeletal muscle only small disturbances of cation activity are found following 10 minutes of ischemia. However, 90 minutes after cessation of blood flow, potassium increases to about 11 mM and sodium decreases to about 30 mM. Under similar conditions, potassium flux in the brain¹² is more pronounced as compared with other tissues.

In summary, cationic fluxes are prominent early during ischemia due to structural changes and modification of the biophysical properties of membranes. These changes can now be detected with electrode systems small enough for potential clinical use. The possibility of monitoring directly specific bio-signals within the microenvironment of capillaries and cells will allow us to detect disturbances at the tissue level as soon as they appear and enable us to decide how far the different compensating mechanisms have been activated. This may be of dramatic importance for the care of the patient. Once the

available reserves have been mobilized, the "point of no return" may have been reached by a minimal, seemingly insignificant deterioration.

Methodology in the field of specific tissue sensors has created many new possibilities for direct and continuous clinical monitoring of different biologic signals in tissue. We are still in the early phase of such investigations. However, the relevance of information provided by such monitoring appears to show great promise, and we need to intensify our efforts to improve and simplify the methods in order to understand better the results of our measurements.

References

1. Ammann D, Pretsch E, Simon W: Darstellung von neutralen, lipophilen Liganden für Membranelektroden mit Selektivität für Erdalkali-Ionen. *Helv Chim Acta* 56:1780-1787, 1973
2. Ammann D, Pretsch E, Simon W: A sodium ion-selective electrode based on a neutral carrier. *Anal Lett* 7:23-32, 1974
- 2b. Ammann D, Bissig R, Cimermann Z, et al.: Synthetic neutral carriers for cations, Ion and Enzyme Electrodes in Biology and Medicine. Edited by Kessler M, Clark LC Jr, Lübbers DW, et al. München-Berlin-Wien, Urban and Schwarzenberg, 1976
3. Bicher HJ, Brulley DF (editors): Oxygen transport to tissues, Instrumentation, Methods and Physiology. New York, Plenum Press, 1973
4. Bicher HJ, Knisely MH: Brain tissue reoxygenation time demonstrated with a new ultramicro oxygen electrode. *J Appl Physiol* 28: 387-390, 1970
5. Bourdeau-Martini J, Odoroff CL, Honig CR: Dual effect of oxygen on magnitude and

- uniformity of coronary intercapillary distance. *Am J Physiol* 226:800-810, 1974
6. Cammann K: Das Arbeiten mit ionenselektiven Elektroden. Berlin, Springer, 1973
 7. Cater DB, Silver IA: Electrodes and microelectrodes used in biology. Reference Electrodes. Edited by Ives DJG, Janz IG. New York, Academic Press, 1961
 8. Clark LC Jr: Monitor and control of blood oxygen tension. *Am Soc Artif Intern Organs* 2:41, 1956
 9. Erdmann W, Kunke ST, Krell W: Tissue P_{O_2} and cell function—an experimental study with multimicroelectrodes in the rat brain. Oxygen Supply. Edited by Kessler M, Bruley DF, Clark LC Jr, et al. München-Berlin-Wien, Urban und Schwarzenberg, 1973
 10. Görmann L, Kessler M: P_{O_2} histograms in regenerating liver tissue. Oxygen Supply. Edited by Kessler M, Bruley DF, Clark LC Jr, et al. München-Berlin-Wien, Urban und Schwarzenberg, 1973
 11. Grote J, Rencau D, Thews G: Oxygen Transport to Tissue. New York, Plenum Press, 1976
 12. Heuser D, Hossmann KA, Schindler U, et al: Changes of cerebral extracellular ion activities and brain volume during prolonged cerebral ischemia and recovery. *Pflügers Arch* 353:99, 1975
 13. Honig CR, Boudreau-Martini J: Extravascular component of oxygen transport in normal and hypertrophied hearts with special reference to oxygen therapy. *Cardiovasc Res* 34/35(11):97-103, 1974
 14. Höper J, Kessler M, Tölke U: Influence of extracellular calcium activity and ion disturbances during no-flow anoxia (ischemia). *Pflügers Arch* 359:132, 1975
 15. Höper J, Kessler M, Simon W: Measurements with ion-selective surface electrodes (pK, pNa, pCa, pH) during no-flow anoxia. Ion and Enzyme Electrodes in Medicine and Biology. Edited by Kessler M, Clark LC Jr, Lübbers DW, et al. München-Berlin-Wien, Urban und Schwarzenberg, 1976
 16. Huckabee WE: Relationship of pyruvate and lactate during anaerobic metabolism: Exercise and formation of O_2 -debt. *J Clin Invest* 37:264, 1958
 17. Jostamdt L, Richter H, Tichai J, et al: Auswirkungen der intraluminalen Druckerhöhung auf die Sauerstoffversorgung des Kaninchenileums und ihre pharmakologische Beeinflussbarkeit. *Langenbecks Arch* (in press)
 18. Kessler M: Normale und kritische Sauerstoffversorgung der Leber bei Normo- und Hypothermie. Habilitationsschrift, Marburg 1968
 19. Kessler M, Lübbers DW: Aufbau und Anwendungsmöglichkeiten verschiedener P_{O_2} -Elektroden. *Pflügers Arch* 291:82, 1966
 20. Kessler M, Grunewald W: Possibilities of measuring oxygen pressure fields in tissue by multiwire platinum electrodes. Oxygen Pressure Recording in Gases, Fluids, and Tissues. Edited by Kreuzer. *Prog Resp Res* 3:147, 1969
 21. Kessler M, Thermann M, Lang H, et al: O_2 -Versorgung lebenswichtiger Organe im Schock mit besonderer Berücksichtigung der Leber, Schock, Stoffwechselveränderungen und Therapie. Edited by Zimmermann WE, Stäblich J. Stuttgart-New York, F. K. Schattauer Verlag, 1970
 22. Kessler M, Lang H, Starlinger H, et al: Aerobic and anaerobic glycolysis in the liver after hemorrhage. Neurohumoral and Metabolic Aspects of Injury. Edited by Kovach AGB, Stoner HB, Spitzer JJ. New York, Plenum Press, 1973
 23. Kessler M, Bruley DF, Clark LC Jr, et al (editors): Oxygen Supply. Theoretical and Practical Aspects of Oxygen Supply and Microcirculation of Tissue. München-Berlin-Wien, Urban und Schwarzenberg, 1973
 24. Kessler M, Lang H, Sinagowitz E, et al: Homeostasis of oxygen supply in liver and kidney. Oxygen Transport to Tissue. Edited by Biehl H, Bruley DF. New York, Plenum Press, 1973
 25. Kessler M, Höper J, Schäfer D, et al: Sauerstofftransport im Gewebe. Klin. Anästhes. Intensivther., Bd. 5: Mikrozirkulation. Edited by Alnefeld FW, Burri C, Dick W, et al. New York, Springer Verlag, 1974
 26. Kessler M, Höper J, Simon W: Methodology and application of a multiple ion selective surface electrode (pH, pK, pNa, pCa) for tissue measurements. *Fed Proc* 33:279, 1974
 27. Kessler M, Schmeling D: Methodology of pH sensitive microelectrodes for intracellular measurements. *Pflügers Arch* 343:64, 1974
 28. Kessler H, Höper J, Hajek K: Multiple ion selective surface and needle electrodes for the measurement of pK, pNa, and pCa. *Pflügers Arch* 355:120, 1975
 29. Kessler M, Bölling B: Methodology of a pH needle electrode. *Pflügers Arch* 359:148, 1975
 30. Kessler M, Clark LC Jr, Lübbers DW, et al (editors): Ion and Enzyme Electrodes in Biology and Medicine. München-Berlin-Wien, Urban und Schwarzenberg, 1976
 31. Kessler M, Messmer K: Tissue oxygenation during hemodilution. *Bibl Haematol* 41: 16-33, 1975
 32. Kessler M, Höper J, Krumme B, et al: Disturbance and compensation of cellular cation activity during anoxia and in shock. Ion and Enzyme Electrodes in Biology and Medicine. Edited by Kessler M, Clark LC Jr, Lübbers DW, et al. München-Berlin-Wien, Urban und Schwarzenberg, 1976
 33. Krogh A: The rate of diffusion of gases through animal tissue, with some remarks on the coefficient of invasion. *J Physiol (Lond)* 52: 391-409, 1918-19
 34. Krumme BA, Strehlau R, Kessler M: Hydrogen clearance measurements on the liver surface

- in situ* with the multiwire electrode. *Arzneim Forsch (Drug Res)* 25:1666-1679, 1975
35. Krumme BA, Strehlau R, Schönlehen K, et al: Redistribution of microcirculation—a new principle of regulation. *Pflügers Arch* 359: 35, 1975
 36. Kunze K: Das Sauerstoffdruckfeld im normalen und pathologisch veränderten Muskel. *Habilitationsschrift*, Giessen, 1967
 37. Lang H, Kessler M, Starlinger H: Die Bedeutung des Lactat/Pyruvat-Quotienten für die Beurteilung der Sauerstoffversorgung der isoliert perfundierten Leber 26. Tagung der Deut. Gesell. Verd. Stoffwechselkrankh., Stuttgart, Oktober 1971
 38. Lang H, Kessler M, Starlinger H: Signs of hypoxia measured by means of P_{O_2} -multi-wire-electrodes by NADH and NADPH fluorescence and determination of lactate and pyruvate formation. *Oxygen Supply, Theoretical and Practical Aspects of Oxygen Supply and Microcirculation of Tissue*. Edited by Kessler M, Bruley, DF, Clark LC Jr, et al. München-Berlin-Wien, Urban und Schwarzenberg, 1973
 39. Lübbers DW, Baumgärtel H: Herstellungstechnik von palladierten Pt-Stichelektroden (1–5 μ Außendurchmesser) zur polarographischen Messung des Wasserstoffdruckes für die Bestimmung der Mikro-zirkulation. *Pflügers Arch* 294:39, 1967
 40. Lübbers DW, Wodick R: Sauerstofftransport im Warmblüterorganismus. *Umschau Wiss Techn* 13:486–492, 1971
 41. Messmer K, Sunder-Plassmann L, Jesch F, et al: Oxygen supply to the tissue during limited normovolemic hemodilution. *Res Exp Med* 159:152–166, 1973
 42. Moody GJ, Oke RB, Thomas JDR: A calcium-sensitive electrode based on a liquid ion exchanger in a poly-vinyl chloride matrix. *Analyst* 95:910–918, 1970
 43. Morf WE, Kahr G, Simon W: Reduction of the anion interference in neutral carrier liquid-membrane electrodes responsive to cations. *Anal Lett* 7:9–22, 1974
 44. Opitz E, Schneider M: Über die Sauerstoffversorgung des Gehirns und den Mechanismus von Mangelwirkungen. *Ergeb Physiol* 46:126–260, 1950
 45. Rink R, Kessler M: Signs of hypoxia in the small intestine of the rat during hemorrhagic shock. *Oxygen Transport to Tissue*. Edited by Bicher III, Bruley DF. New York, Plenum Press. *Adv Exp Med Biol* 37A:469–475, 1973
 46. Schönlehen K, Krumme BA, Bünte H, et al: Kontrolle der Intensivbehandlung durch Messung von Mikro-zirkulation und O_2 -Versorgung. *Langenbecks Arch Suppl Chir Forum* 72–76, 1976
 47. Siesjö BK, Johansson H, Norberg K, et al: Brain function, metabolism and blood flow in moderate and severe arterial hypoxia. *Brain Work, the Coupling of Function, Metabolism and Blood Flow in the Brain*. Edited by Ingvar DH, Lassen NA. Copenhagen, Munksgaard, 1975
 48. Sinagowitz E, Baker R, Strauss J, et al: Renal tissue oxygenation during hypoxic hypoxia. *Oxygen Transport to Tissue*. Edited by Grote J, Reneau D, Thews G. New York, Plenum Press, 1976
 49. Sinagowitz E, Hagist R, Sommerkamp H: Measurements with surface electrodes for interstitial ion activities and local tissue P_{O_2} on the human kidney (preliminary report). *Ion and Enzyme Electrodes in Biology and Medicine*. Edited by Kessler M, Clark LC Jr, Lübbers DW, et al. München-Berlin-Wien, Urban und Schwarzenberg, 1976
 50. Sinagowitz E, Kessler M: Standardization of producing needle electrodes. *Oxygen Transport to Tissue*. Edited by Bicher III, Bruley DF. New York, Plenum Press. *Adv Exp Med Biol* 37A:23–27, 1973
 51. Sinagowitz E, Rahner H, Rink R, et al: Local oxygen supply in intra-abdominal organs and in skeletal muscle during hemorrhagic shock. *Oxygen Transport to Tissue*. Edited by Bicher III, Bruley DF. New York, Plenum Press. *Adv Exp Med Biol* 37A:505–511, 1973
 52. Sinagowitz E, Rahner H, Rink R, et al: Die Sauerstoffversorgung von Leber, Pankreas, Duodenum, Niere und Muskel während des hämorrhagischen Schocks. *Langenbecks Arch Chir Suppl Chir Forum* 301–303, 1974
 53. Starlinger H, Lübbers DW: Polarographic measurements of the oxygen pressure performed simultaneously with optical measurements of the redox state of the respiratory chain in suspensions of mitochondria under steady state conditions at low oxygen tension. *Pflügers Arch* 341: 15, 1973
 54. Suwa N, Takahashi T: Morphological and Morphometrical Analysis of Circulation in Hypertension and Ischemia. Edited by Büchner F. München-Berlin-Wien, Urban und Schwarzenberg, 1971
 55. Thews G: Die Sauerstoffdiffusion im Gehirn. *Pflügers Arch* 271:197–226, 1960
 56. Whalen W, Riley J, Nair P: A microelectrode for measuring intracellular P_{O_2} . *J Appl Physiol* 23:789, 1967